

MR-based Attenuation Correction of Local Radiofrequency Surface Coils in PET/MR Hybrid Imaging

Daniel H. Paulus¹, Harald Braun¹, Bassim Aklan¹, and Harald H. Quick¹

¹Institute of Medical Physics, Friedrich-Alexander-University Erlangen-Nuremberg, Erlangen, Bavaria, Germany

Target Audience: Researchers and physicians who are working in the new field of PET/MR hybrid imaging.

Purpose: In simultaneous PET/MR imaging, local receiver surface radiofrequency (RF) coils are positioned in the field-of-view (FOV) of the PET detectors and potentially attenuate and scatter the PET annihilation photons. For the patient table and rigid coils, where the geometry and position are fixed, pregenerated 3D attenuation maps (μ -map) can be used for PET attenuation correction (AC) [1]. However, flexible RF surface coils placed on the top of the patient's body can vary in position and geometry during the examination. Since RF coils are not inherently visible in MR images [2], AC of flexible RF coils is an unsolved problem and they are thus currently omitted in PET AC. With up to four body matrix RF coils being used in the standard whole-body PET/MR protocol, attenuation of these coils is a non neglectable factor. In this work, the effect of local receiving RF coils used in the Biograph mMR hybrid PET/MR system on PET emission data was quantified and a first approach for CT-based AC is presented.

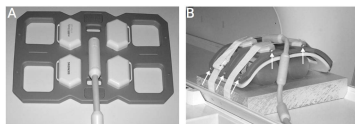


Fig. 1: (A) Body matrix RF coil, (B) phantom setup: RF coil was fixed on the top of two cylindrical bottles and 12 cod liver oil capsules were attached to the surface of the coil (arrows).

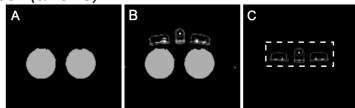


Fig. 2: Transaxial slice of: (A) MR-based Dixon-VIBE μ -map of the phantom fluid, (B) μ -map of MR-based (phantom) and CT-based (RF coil) μ -map, and (C) CT-based μ -map of only the middle part of the RF coil (dashed rectangle) used for the patient scan.

Materials and Methods: All measurements were performed on a Biograph mMR system (Siemens AG, Healthcare Sector, Erlangen, Germany), a hybrid whole-body PET/MR system that consists of a 3.0 T MR scanner with a fully integrated PET unit in its magnet isocenter. The μ -maps of the flexible 6-channel body matrix RF coil (Fig. 1A) were based on CT images and have been converted from CT energy to 511 keV by using the bilinear conversion proposed by Carney [3].

For the phantom measurements, two uniform cylindrical plastic bottles filled with phantom fluid and ¹⁸F (84.1 MBq) were placed parallel side-by-side on a styrofoam block and the body matrix RF coil was fixed on the top of the two bottles. For the image registration between MR and CT images, 12 cod liver oil capsules have been attached on the surface of the coil (Fig. 1B). Two different PET emission scans were performed consecutively, one with and the other without the body matrix RF coil placed on the top of the phantom. To simulate PET/MR scanning conditions, AC of the water filling was performed by the scanner based on a 3D FLASH Dixon-VIBE MR sequence (Fig. 2A). After image registration, the following PET images were reconstructed: (1) PET reference scan without RF coil, (2) PET scan with coil, but omitting the RF coil in AC (current PET/MR scanning conditions), and (3) CT-based AC of the coil (Fig 2B), where the markers were used for image registration, which were visible in both image modalities, MR and CT.

In addition to the phantom scans, a 45-year old female patient with a known neuroendocrine carcinoma of the pancreas was scanned with and without the body matrix RF coil. AC of the human body was based on a Dixon-VIBE MR sequence, provided by the scanner. For AC of the RF surface coil, only the rigid middle part (Fig. 2C) was used due to the missing information about the exact shape of the flexible outer part.

Results: The overall loss of true counts in the phantom scan due to the presence of the body matrix RF coil was calculated to be around 4.7% in the phantom scan and 4.4% in the patient scan. To evaluate the results precisely, small region of interests (ROI) were defined inside the two bottles (Fig. 3A) and plotted for each slice as illustrated in Fig. 3B. The graphs show the percentage difference of the PET scans without AC of the coil (Fig. 3C) and with AC of the RF coil (Fig. 3D) compared to the reference scan.

In Fig. 4A the whole-body PET emission image of the patient is shown that illustrates the lesion in the abdominal area (black arrow). For quantitative evaluation, a line profile was drawn through the center of the lesion (Fig. 4B). The corresponding graph, showing the activity concentration along this profile is given in Fig. 4C.

Discussion: The overall loss of true counts caused by the body matrix RF coil was calculated to be rather small with values around 4.5%. Looking at the PET emission images in more detail, we found that the effect of the flexible RF surface coil is location-dependent (Fig. 3C). The closer the ROI is located to the RF coil (#1, 2, and 6), the higher is the effect of the RF coil on the activity concentration with a difference up to 15%. This is due to the fact that the likelihood of annihilation photons being attenuated or scattered is higher near the coil, a solid angle effect.

If CT-based AC of the RF coil is applied, a slight overcorrection of the PET activity concentration compared to the reference can be observed. This might be caused by artifacts in the CT images around strongly attenuating materials and by a bias of the conversion from Hounsfield units to linear attenuation coefficients at 511 keV, which is optimized for human body and not for the materials of MR hardware components. Looking at the line profile of the patient scan, the loss of activity concentration due to the RF coil (difference between blue and red line) could be compensated with AC of the rigid parts of the otherwise flexible RF coil (green line matches blue line).

Conclusion: Disregarding local RF coils in PET AC can lead to a bias of the PET AC images that is regional dependent. The closer the analyzed region is located to the attenuating parts of the RF coil, the higher the bias. To compensate the attenuation of the local RF coil, markers can be used for position determination to apply CT-based AC, which shows good results in the phantom study as well as in the patient study.

References: [1] Quick et al. MAGNETOM Flash 2011, 1, 80-100, [2] Paulus et al, Med. Phys. 2012, 39(7), 4306-4315, [3] Carney et al. Med. Phys. 2006, 33(4), 976-983

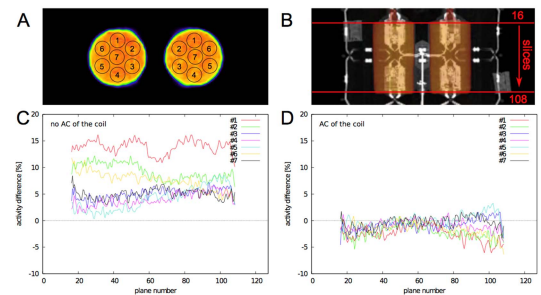


Fig. 3: (A) Axial PET image of the cylindrical bottles with 7 circular ROIs. (B) Illustration of the relative position of RF coil, bottles, and the range of axial planes plotted in the graphs. (C/D) Percentage difference of the mean intensity of each ROI between the reference scan and the PET image without AC of the coil (C) and with AC of the coil (D). While the RF coil caused attenuation by about 2-15% (C), AC of the RF coil almost completely compensated for this attenuation (D).

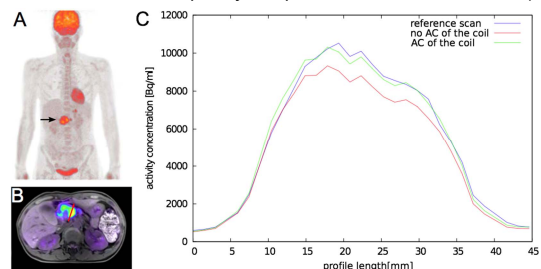


Fig. 4: (A) MIP of the PET only image of the patient that shows the lesion with high tracer uptake (arrow). (B) Line profile through the center of the lesion. (C) Plot of the activity distribution of the line profile for all three PET images: 1) without RF coil (blue), 2) with RF coil and no AC (red), and 3) with RF coil and AC applied.